The Identification of impulsive noise in HFC networks use Wavelets

SUZENE FAUSTO and ALDO ARTUR BELARDI
Electrical Department
Centro Universitário da FEI
Av. Humberto de Alencar Castelo Branco ,3972
São Paulo, BRAZIL
suzenefausto@fei.edu.br and belardi@fei.edu.br

Abstract - This paper developed a methodology for the use of wavelets for the identification of impulse noise in the frequency range of the feedback network Hybrid Fiber-Coaxial (HFC), and a method for analyzing the energy spectrum. Networks (HFC) Cable television (CATV) has been established as an important infrastructure to provide interactive content and broadband access on the World Wide Web, Internet bandwidth. HFC networks are increasingly required in the aspects of quality and ability to carry digital signals due to the availability of transmission bandwidth and coverage in your service area and leave being only networks which television channels besides the noises that interfere with services provided by the operator. The impulsive noise in the frequency range of return becomes one of the main problems faced by operators, for his interference in carriers of Cable Modems (CM), because loss of information transmitted and even unavailability of services.

Keywords: HFC Networks, Impulsive Noise, Wavelets

1. Introduction

In HFC networks, impulsive noise in the frequency range of return is one of the main problems faced by operators, this noise interferes with carriers of "Cable Modems", causing loss of information transmitted and even unavailability of services. The impulsive noise is to peak amplitude signals entering generally high across the spectrum of the return channel and causes very strong at the entry level, signal-to-noise amplifiers and laser momentary an increase which makes the electro-optical conversion return. Are initially characterized by having a behavior similar to a sine wave, with peak values exponentially decaying, lasting a few seconds and the time between occurrences time can vary from several minutes up to 100 us[1].

This type of noise has its origin in various sources, such as discharges in electric distribution networks, often located on the same poles conductors discharge network cable connector contacts between oxidized and even appliances. Dividing the spectrum is shown in Figure 1. This area is very susceptible to impulse noise because it is a low frequency region where there are several emission sources in the environment, such as the microwave oven, electric shower reactor fluorescent lamp, etc. Other types of noise, and impulsive, may also join in the frequency range of return, such as short-wave carrier transmitted by amateur radio or even problems with equipment in the network itself.

Fig. 1 - Division of usage frequency in HFC networks

The "headend" is responsible for obtaining the channels from the satellites, open channels already available for reception venue or closed channels, and nationalities from different sources [2] [3].

The transport network initiates the "headend" through optical transmitters, which are responsible for sending the signal through the optical fiber until the installed receivers in the network outside.

This bidirectional network has the ability to traffic data in both directions simultaneously, the network comprises two optical links, one for transmission of data traffic from the "headend" to the subscribers and one for transmitting data traffic subscribers to the "headend", called the path of return.

The backbone network differs through strategically in the distribution of RF signals via coaxial network where no signal splitter to meet subscriber is installed.

This type of network is limited to only transmit signals between the amplifiers, which are called trunk amplifiers.

The service network differs from the distribution network, as it is this network that shunts are installed to service subscribers [4] [5] [6].

The internal network is the network portion that is in the subscriber environment, from the derivation of the service network for the device to decode TV channels.

Due to its location being in an uncontrolled environment and with multiple points of open network, is where most noise problems entering the network, around 90% occurs.

The increasing demand for bandwidth is increasingly demanding the use of the frequency of the operators of cable TV spectrum [7][8].

Currently network uses 1002MHz, and 1GHz, in the direct path. The increased use of the spectrum comes add more channels, digital or analog, available for use.

The path of return has a limited frequency spectrum, originally from 5 to 42MHz and currently of 5MHz to 82MHz wide [9] [10] [11] [12].

2. The Wavelets

The wavelet can be defined as a waveform of limited duration and with a mean value equal to zero. The wavelet behaves like a sine wave, which is the basis of time series analysis Fourier Transform [13].

The sinusoids have typically smooth and predictable behavior, but the wavelets differ by presenting irregular and asymmetrical shape, can be functions, or windows, both with compact support in the frequency domain and time domain. They are used to separate the signal into parts while maintaining the resolution of each of the components connected to the scale used [14].

We can define the wavelets are functions of finite energy and can be used very effectively to represent signals of short duration in the time domain and sometimes only a finite number of coefficients are required to represent a complex signal.

The analysis using the wavelet has been a good alternative to replace the classical analysis using Fourier series, especially in the analysis of signals, interpretation of seismic signals and also in the solution of numerical methods applied in electrostatics and electromagnetism [15] [16] [17].

In general wavelets may be defined by:

$$\psi_{a,b}(x) = |a|^{-\frac{1}{2}} \psi\left(\frac{x - b}{a}\right) \quad a, b \in R, a \neq 0 \tag{1}$$

Some types of wavelets are mentioned in the literature and can build them from other families of templates that are adapted more appropriately for each case.

In Figure 2 we show the Morlet wavelet modulated Gaussian or which is formulated by:
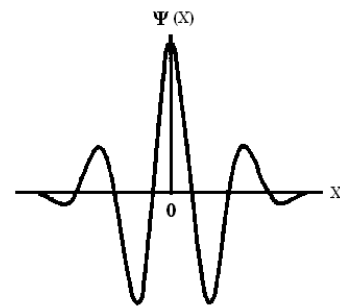
$$\psi(x) = e^{i\omega_0 x} e^{-x^2/2} \tag{2}$$

Fig. 2 - Morlet

In Figure 3 presents the wavelet known as Mexican Hat and have your equation given by:
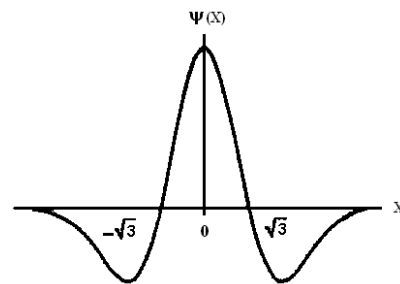
$$\psi(x) = (1 - x^2)e^{-x^2/2} \tag{3}$$

Fig. 3 - Mexican Hat

In Figure 4 we show the Shannon wavelet and its formulation is given by:

$$\psi(x) = \frac{\sin(\frac{\pi x}{2})}{\frac{\pi x}{2}} \cos(\frac{3\pi x}{2})$$

$$\varphi(x) = \begin{cases} \dfrac{\sin(\pi x)}{\pi x}, & x \neq 0 \\ 1 & , \quad x = 0 \end{cases} \tag{4}$$
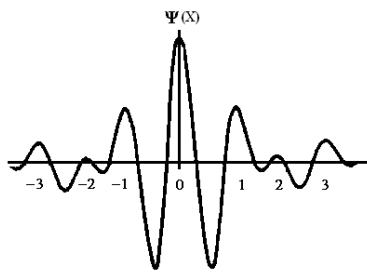
Fig. 4 - Shannon

The Haar wavelet is one of the most well-known for its very simple. It has only two coefficients of filters, so a long-range transition is guaranteed. The parties that sometimes can become more suitable analyze a constant signal. The Haar wavelet function is represented by a square wave according to Figure 5. Concerning the computational effort by the fact result in sparse matrix is ideal for real-time processing.
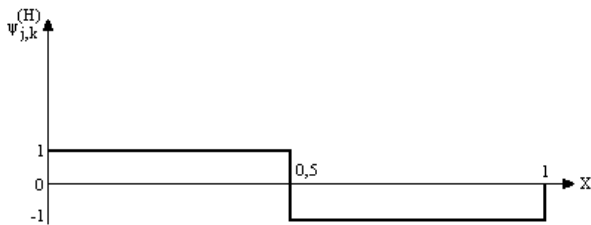

Fig. 5 - Haar function in the range from 0 to 1

The Haar wavelet for example is defined by two families of wavelet, the mother and father, the latter being represented by ϕ scale called function is defined by:

$$\phi^{(H)}(x) = \begin{cases} 1 & 0 \le x < 1 \\ 0 & \text{otherwise} \end{cases} \tag{5}$$

Thus there are other types such as Daubechies wavelet, Symmlet, Gaussian density, de Oliveira, etc. [18][19].

3. Modeling of Signs

Due to the difficulty of withdrawing samples generated by the hardware perform the mathematical model, which consists in producing samples of RF signals comprising the article of this study. It is important to note that at this time it is a discrete sample and not continuous, has points defined and finite. The study of the spectrum range is 5 to 50 MHz and the sampling rate is 100 MHz because, according to the Nyquist theorem described above, the sampling rate must be at least twice the highest frequency that the analog signal can reach. The following signals were modeled [20]:

3.1) Figure 6 shows the signal carrier 16QAM as a function of time and frequency modulated in the central 30MHz.
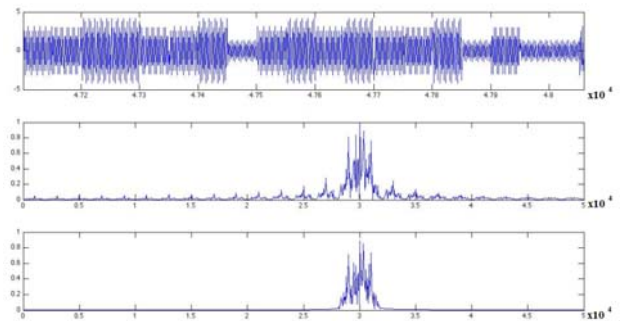

Fig. 6 - Carrier 16QAM

3.2) To model the noise floor a function that generates random numbers of normal distribution was used. In the Figure 7 graph resulting from the noise model as a function of time is shown. In Figure 8, shown is presented FFT of the same signal.
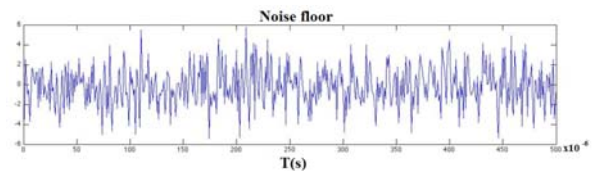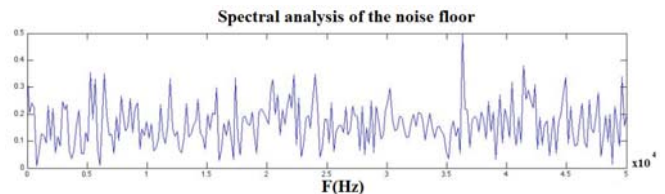

Fig. 7 - Noise a function of time

Fig. 8 - FFT noise

3.3) In the modeling of impulsive noise, the sine function to create various carriers in harmonic frequencies that simulate a source of impulsive noise was used. The combination of these carriers is added to the other signals in the model. In Figure 9 we show the carriers that make up the impulse noise as a function of time, presented in Figure 10 the combined carrier or impulsive noise as a function of time and Figure 11, the FFT transform of the impulse noise [21].
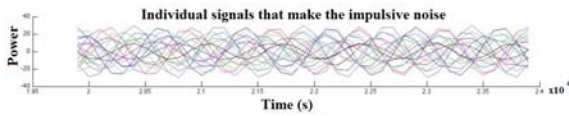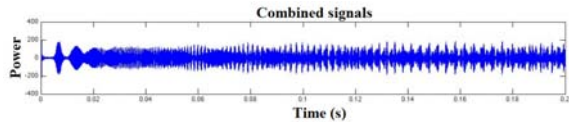
Fig. 9 - Noise of carrier
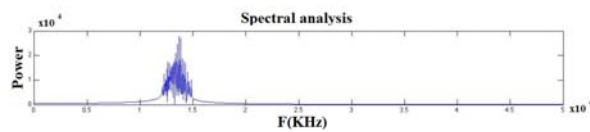

Fig. 10 - Combined carriers

Fig. 11 - FFT transform

The Figure 12 shows the final model with the carrier 16QAM, the noise floor and the combined impulse noise.
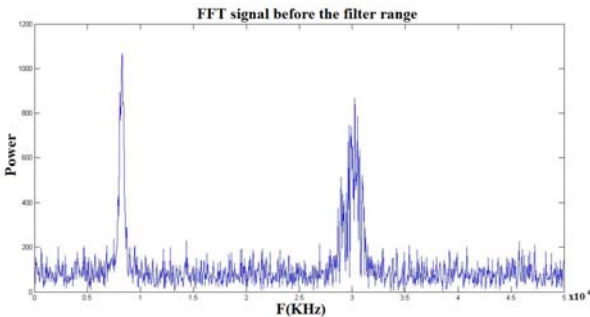

Fig.12 - Final modeling

We conducted a pre-treatment at the end of modeling that is to remove the patterned sample spectrum of the carrier 16QAM, assuming it is not a sound, but of information or data from the "cable modem" installed in subscribers. To remove the carrier applied a band reject filter centered at 30 MHz and 3.2 MHz bandwidth [22] [23].

With the patterned samples, three methods to the study of the identification of impulsive noise, or calculating the energy of the secondary samples in the time domain, the calculation of the energy of the wavelet coefficients, analysis scalogram obtained by applying the wavelet been developed. For the study of the first two methods, the primary sample is submitted, to a bank of filters composed of 44 digital band pass filters, which segments the primary sample in 44 secondary samples with a width of 1 MHz of spectrum, as shown in Figure 13 [24].
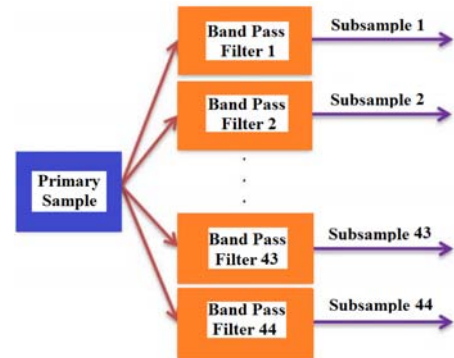

Fig.13 - Application of filter bank

4. Formulation

4.1) Direct energy calculation

This method is called direct energy calculation, for calculating the energy of the signal is carried directly in the time domain the output of the filter bank, and the calculated energy E_j of the sub-sample, $A_{i,j}$ the value of the sub sample j in an instant i.

$$E_j = \sum_{i=1}^{n} A_{i,j}^2 \tag{6}$$

From the calculation of the energy value is then checked against a threshold value calculated by the following equation, and Th_{M1} the threshold value and the calculated energy E_j of the subsample j.

$$Th_{M1} = \frac{1}{n} \sum_{j=1}^{n} E_j \tag{7}$$

For detection of the peaks of energy is subtracted from the value of the threshold value E_j, $P1_j$ and a vector that stores the result of the detection of the peaks of energy, the energy E_j calculated from the subsample j e Th_{M1} the threshold value.

$$P1_j = \left[E_j - Th_{M1} \right]_{j=1}^{n} \tag{8}$$

The Figure 14 shows the calculation of the energy and direct comparison with a threshold.
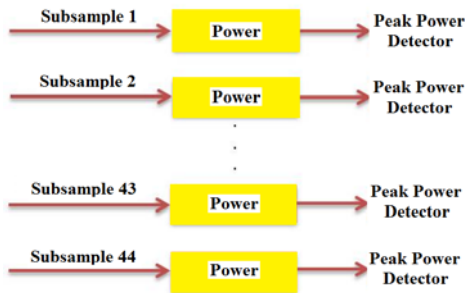
Fig.14 - Direct energy calculation

4.2) Energy calculation with the wavelet coefficients

The wavelet transform is applied to each of the 44 sub-samples and each subsample results in two die sets, or coefficients, as shown in Figure 15 and approach the coefficients A_j and D_j The coefficients of the detail subsample j.
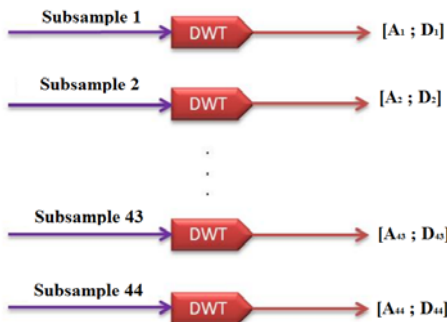

Fig.15 - Application in the subsamples

In this article various types of wavelets through Matlab application, such as Haar, Mexican hat Gauss, Daubechies and Symmlets were used, with the aim of verifying the shorter execution time between them. The results obtained are shown below. With the obtained coefficients, the energy of each set of coefficients is calculated, and Ea_j energy approximation coefficients $A_{j,i}$ the approximation coefficients of the subsample i and j.

$$Ea_j = \sum_{i=1}^{n} A_{j,i}^2 \qquad (9)$$

A new vector was developed as, M_j being the vector containing the average of the sum of the energies of the coefficients of approximation and details of the sub-sample j, Ea_j energy coefficients approach j and subsample Ed_j energy coefficients details of the sub-sample j.

$$M_j = \frac{Ea_j + Ed_j}{2} \qquad (10)$$

Similar to the previous method, in Figure 16, it is found the value of this energy against a threshold value, considering now that the vector contains the average sum of the energies of the coefficients of approximation and detail.
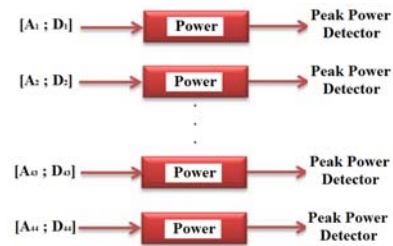

Fig.16 - Applying the subsamples

4.3) Analysis by scalogram

This third method is based on analysis using scalogram obtained from the result of the application of wavelet in the primary sample, without the need for segmentation of the filter bank, which causes a reduction in the computational time of sample processing. A table that relates the position of scale as a function of frequency of the wavelet used is calculated. It consists of three axes x represents time, y and z that represent the scale that represents the value of the coefficient. The z axis is usually displayed in a range of colors or brightness.

5. Results

For calculating direct energy perform the calculation of the signal energy in the time domain directly to the output of the filter bank, and the energy of each sub-sample which results in a vector of 44 positions is calculated, as shown in Figure 17 [25].

$$E_j = 1*10^5*[0,0938\ 0,0896\ 0,2835\ 4,2337\ ::::$$
$$::: 0,0925\ 0,0936\ 0,0931\ 0,0902]_{1x44} \qquad (11)$$

At this moment from the threshold value, which result in a new vector. For the final results, negative values are replaced by zero in accordance with Figure 18.

For the method two for the wavelet transform is applied the output of the filter bank in each subsamples. This new process results in two new matrixes, one with the coefficients of approximation and another with the detail coefficients.
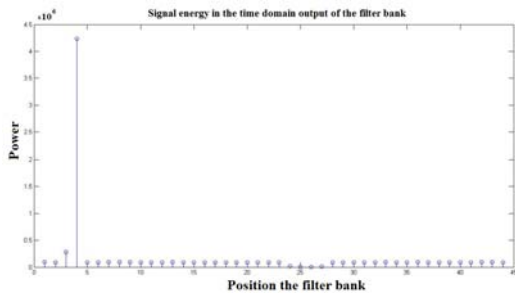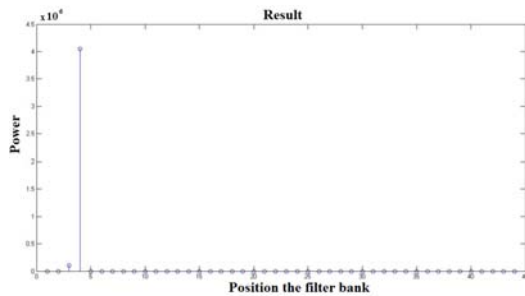
Fig.17 - Calculation of direct energy

Fig.18 - End result with direct energy

$$A_{j,i} = \begin{bmatrix} 0,0188 \times 10^{-6} & 0,1512 \times 10^{-6} & \ldots & 0,1434 & 0,2589 \\ 0,0167 \times 10^{-6} & 0,0042 \times 10^{-6} & \ldots & 0,7544 & 0,7008 \\ . & . & . & . & . \\ . & . & . & . & . \\ 0,0733 \times 10^{-7} & 0,1720 \times 10^{-7} & \ldots & 0,0329 & 0,0320 \\ -0,2733 \times 10^{-7} & -0,6539 \times 10^{-7} & \ldots & -0,0073 & -0,0064 \end{bmatrix}_{44 \times 50.000} \quad (12)$$

$$D_{j,i} = \begin{bmatrix} -0,1311 \times 10^{-7} & -0,5709 \times 10^{-7} & \ldots & -0,0471 & -0,0094 \\ -0,0770 \times 10^{-6} & 0,1636 \times 10^{-7} & \ldots & -0,0485 & 0,0740 \\ . & . & . & . & . \\ . & . & . & . & . \\ -0,0815 \times 10^{-8} & -0,4499 \times 10^{-8} & \ldots & 0,0999 & -0,0308 \\ 0,0794 \times 10^{-7} & 0,1720 \times 10^{-7} & \ldots & 0,0018 & 0,0299 \end{bmatrix}_{44 \times 50.000} \quad (13)$$

Which results in Figure 19 is the energy of the coefficients of approximation and Figure 20 is the energy of the coefficients details.
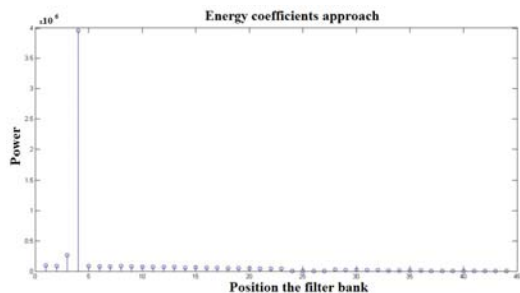

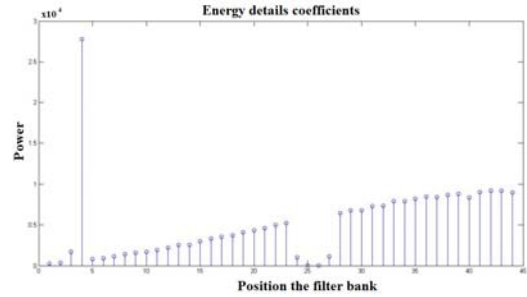Fig. 19 - Energy coefficients approach

Fig. 20 - Energy details coefficients

As each vector stores some of the energy spectrum, we calculated the arithmetic mean of the two vectors formed by the previous results, the average energy resulting from the sum of the coefficients of approximation and details as shown in Figure 21.
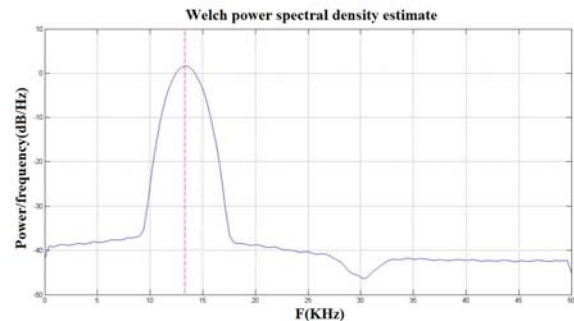

Fig. 21 - Energy average of the sum of the coefficients

In the same way as described above it is possible to calculate the threshold value by making the substitution of negative values with zero. The scalogram in the wavelet transform is applied directly to the impulsive signal without the use of the filter bank. As we found in the literature a methodology that tell us what the best wavelet function to be used in a particular type of signal, we used a comparative way through the Wavelet Toolbox of Matlab, Gauss2, Gauss4 and Mexican Hat have greater similarity to our kind signal. The estimated power spectral density is shown in Figure 22.
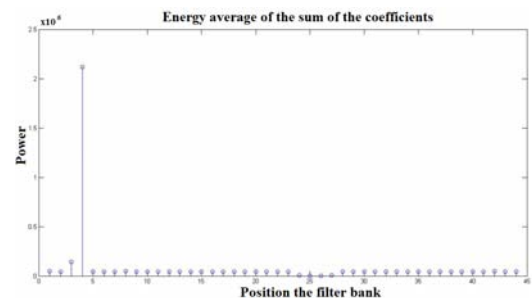

Fig. 22 - Welch power spectral density estimate

The application of the wavelet Gauss2 results in a matrix in which it is located the coefficient of higher value and thus determined the line you are on the scale of this coefficient. It is possible to improve the accuracy of this method by reducing the pitch between the scale levels or the use of wavelets higher

levels, although both alternatives increase the computational time. With the use of the wavelet Gauss4 has the result shown in Figure 23.
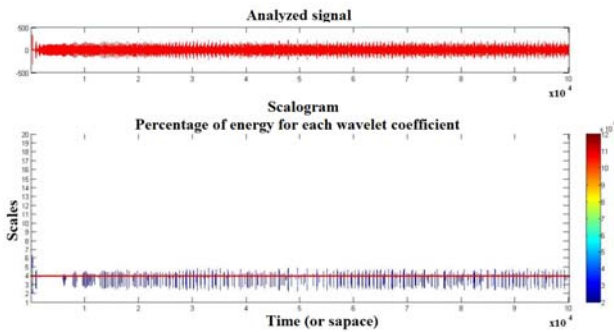

Fig. 23 - The estimated power spectral density

In Tables I and II present the results of the execution time of the application of three different methodologies.

Table I - Computational time by the method of direct energy and the coefficients of the wavelet

	Runtime (s)	
Sample	Direct energy	Energy coefficients with wavelets
1	2,52971	2,92477
2	2,67219	3,07896
3	2,54940	2,93373
4	2,59438	2,98802
.	.	.
.	.	.
.	.	.
15	2,48999	2,87541
16	2,51136	2,89538
17	2,49003	2,87230
18	2,61232	2,99627
19	2,50685	2,87976
20	2,50476	2,87464

Table II - Computational time using the wavelet directly on the estimated power spectral density

	Runtime (s)	
Sample	Gauss2	Gauss4	MexH
1	0,33808	0,33953	0,38265
2	0,35639	0,34460	0,37402
3	0,36655	0,33682	0,36659
4	0,34754	0,33576	0,37717
5	0,34111	0,33277	0,36816
.			
.			
.			
15	0,34944	0,33507	0,37377
16	0,33624	0,34229	0,37441
17	0,34034	0,34708	0,38206
18	0,33037	0,33580	0,37949
19	0,34384	0,33711	0,37420
20	0,34375	0,34388	0,38665

The Figure 24 shows a graph comparing the runtime of the three methodologies adopted.
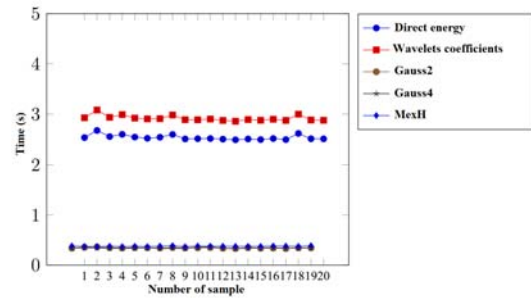

Fig. 24 - Runtime between the three methodologies

6.Conclusion

The present study has made possible the expansion of production and knowledge across the importance of contributing to the area of Signal Processing that evidenced two distinct subjects, HFC Networks and Wavelets.

The greatest difficulty is the inability to measure, in real environment, samples of impulse noise because of its random characteristics of occurrence for this type of noise has a short duration and is unpredictable because it depends on natural or artificial factors cannot be controlled. We also have to take into consideration that a insertion of noise in real HFC network is prohibitive as it may harm the subscriber is illegal. The pretreatment of each sample removed the carrier 16QAM which has its origin in the network equipment, so it has become possible to identify the impulsive noise.

Three Methods were developed for identifying the impulsive noise and the first method was used in this work as a comparative for the second and third methods.

The second method was the first attempt to identify the impulsive noise and was the starting point for understanding the computational costs involved in the application of transformed wavelet. For the second method the level of details of the sample decomposition by the transformed wavelet is not an important parameter and, therefore, the simple Wavelet as the Haar is as efficient as one Wavelet Symmlet of the eighth level, the impacting factor being that the computational cost varies with the wavelet used.

The third method, analysis using scalogram, was the one which demonstrated the best computational time compared to the previous ones. This was possible because the third method does not require the use of the stage segmentation of the sample by the bank of digital filters. This method presented a computational time 86.58% lower to the first method and 88.35% lower to the second method.

The practical advantage of using this process in a CATV operation is the detection of these impulsive noises in return lines, and with it, schedule preventive maintenance on the HFC network, which improves the quality of services provided by the operator.

REFERENCES

[1] Tunmann E. O., Hybrid fiber-Optic Coaxial Networks,Ed. Flatiron Publishing, 1995.

[2] Fonseca A. et al, "Serviços suportados em redes HFC," Communication Technology, v. 1, n°1, 2010.

[3] Alencar M. S., Televisao Digital,Ed. Erica, 2012. R. Wolters, "Characteristics of upstream channel noise in CATV networks," IEEE Transactions on Broadcasting, v. 42, n°4, pp. 328-332, 1996.

[4] Zhang L. et al, "Research of the noise characteristic on the upstream channel for HFC network," IEEE, 2° International Conference on Signal Processing Systems, ICPS, v. 2, pp. 422-426, 2010.

[5]Jiarong H., Z. Ying, Y. Guojun, "Analysis of VOD technology and the noise in transmission channel of HFC," IEEE Information Technology an Applictions, IFITA'09, v. 2, pp. 424-427, 2009.

[6]Robin M., Poulin M., Digital television fundamentals, 2nd ed., Ed. McGraw-Hill, 2000.

[7] Miller J., Thomas J., "The detection on signals in impulsive noise modeled as a mixture process," IEEE Transactions on Communications, v.24, n°5, p. 559-563, 1976.

[8]Eldering C. A., Himayat N., Gardner F. M., "CATV return path characterization for reliable communications," IEEE Communications Magazine, v.33, n° 8, pp. 62-69, 1995.

[9] Jacobsen K. S., Bingham J. A., Cioffi J. M., "Synchronizes DMT, for multipoint to point communications on HFC networks," IEEE Global Telecommunications Conference, Globecom 95, v.2, pp. 963-966, 1995.

[10] Openheim A. V. et al, Discrete time signal processing, Ed. Prentice Hall, 1999.

[11] Tsihrintzis G. A., Nikias C. L., "Performance of optimum and suboptimum receivers in the presence of impulsive noise modeled as an alpha-stable process," IEEE Transactions on Communications, v.43, n° 234, pp. 904-914, 1995.

[12] Fausto S., "Utilização de Wavelets para identificação do ruído impulsivo na faixa de frequência de retorno em redes HFC", Master's Dissertation, 2014.

[13] Morettin, P. A. Ondas e Ondaletas: da Análise de Fourier à Análise de Ondaletas, Edusp, 1999.

[14]Malvar, H. S.; Staelin, D. H. The lot: Transform coding without blocking effects. Acoustics, Speech and Signal Processing, IEEE Transactions, v.37, n°4, pp. 553-559, 1989.

[15]Meyer, Y. Wavelets-algorithms and applications. Wavelets-Algorithms and applications Society for Industrial and Applied Mathematics Translation,1993.

[16]Daubechies, I. Orthonormal bases of compactly supported wavelets. Communications on pure and applied mathematics, 1988. Wiley Online Library, v.41, n°7, pp. 909-996, 1988.

[17] Daubechies, I. The wavelet transform, time-frequency localization and signal analysis. Information Theory, IEEE Transactions, v.36, n°5, pp. 961-1005, 1990.

[18]Oliveira, H. de; Falk, T.; Távora, R. Decomposição de wavelets sobre corpos finitos. Rev. da Soc. Bras. de Telecomunicações, pp. 38-47, 2002.

[19]Oliveira, H. M. ; Soares, L. R.; Falk, T. H. A family of wavelets and a new orthogonal multiresolution analysis based on the Nyquist criterion. Revista da Sociedade Brasileira de Telecomunicações, 2003.

[20]Degardin, V. et al. Classification and characterization of impulsive noise on indoor powerline used for data communications. Consumer Electronics, IEEE Transactions v.48, n°4, pp. 913-918, 2002.

[21]Jacobsen, K. S.; Bingham, J. A.; Cioffi, J. M. Synchronized dmt for multipoint-to-point communications on HFC networks. IEEE. Global Telecommunications Conference, 1995.

[22]Wolters, R., Characteristics of upstream channel noise in CATV-Networks. Broadcasting, IEEE Transactions, v. 42, n°4, pp. 328-332, 1996.

[23]Zhang, L. et al. Research of the noise characteristic on the upstream channel for HFC Network. In: IEEE. Signal Processing Systems (ICSPS),2nd International Conference, 2010.

[24]Liang, J.; Elangovan, S.; Devotta, J. A wavelet multiresolution analysis approach to fault detection and classification in transmission lines. International Journal of Electrical Power & Energy Systems, Elsevier, v. 20, n°5, pp. 327-332, 1998.

[25]Palm, W., Introduction to Matlab 7 and Simulink for Engineers, McGraw-Hill, pp. 55-97, 2003.